The dynamics of vapor bubbles in acoustic pressure fields

Y. Hao and A. Prosperetti
Department of Mechanical Engineering, The Johns Hopkins University, Baltimore, Maryland 21218

In spite of a superficial similarity with gas bubbles, the intimate coupling between dynamical and thermal processes confers to oscillating vapor bubbles some unique characteristics. This paper examines numerically the validity of some asymptotic-theory predictions such as the existence of two resonant radii and a limit size for a given sound amplitude and frequency. It is found that a small vapor bubble in a sound field of sufficient amplitude grows quickly through resonance and continues to grow thereafter at a very slow rate, seemingly indefinitely. Resonance phenomena therefore play a role for a few cycles at most, and reaching a limit size—if one exists at all—is found to require far more than several tens of thousands of cycles. It is also found that some small bubbles may grow or collapse depending on the phase of the sound field. The model accounts in detail for the thermo-fluid-mechanic processes in the vapor. In the second part of the paper, an approximate formulation valid for bubbles small with respect to the thermal penetration length in the vapor is derived and its accuracy examined. The present findings have implications for acoustically enhanced boiling heat transfer and other special applications such as boiling in microgravity. © *1999 American Institute of Physics.* [S1070-6631(99)02208-4]

I. INTRODUCTION

Acoustic cavitation has provided a strong incentive for the study of the dynamics of gas bubbles in oscillating pressure field (see, e.g., Refs. 1–3), but the understanding of the corresponding problem for vapor bubbles is, relatively speaking, less developed.

In practice, oscillating vapor bubbles are encountered in acoustic cavitation in cryogenic liquids,[4,5] the propagation of pressure waves and shocks in boiling channels (see, e.g., Refs. 6–8), and acoustically enhanced boiling heat transfer (see, e.g., Refs. 9–13).

More recently, it has been proposed that acoustic radiation forces may be used to remove bubbles from heated surfaces in microgravity,[14] thus avoiding the premature boiling crisis typically encountered in such conditions (see, e.g., Refs. 15 and 16). It is well known that the direction of these forces depends on whether the bubble is driven above or below resonance. The resonance properties of vapor bubbles therefore determine the appropriate frequency range for this application. Early papers on the subject[17–19] reported the apparent existence of two resonant radii for a given sound frequency, an intriguing aspect that has been subsequently studied by Marston and Greene,[20] Marston,[21] Khabeev,[22] Nagiev and Khabeev,[23] and others.

Most of the theoretical work was carried out analytically under the severe restriction of linear or weakly nonlinear oscillations, and it is not clear how the features that it brought to light would affect the motion of vapor bubbles under strong forcing. It is the purpose of the present study to carry out a numerical investigation of this regime of oscillation comparing the results with the predictions of earlier analytical theories.

II. MATHEMATICAL FORMULATION

Even with the assumption of sphericity, the complete problem of a vapor bubble undergoing nonlinear radial pulsations in a sound field is a complex problem, as its exact solution requires a consideration of the equations of conservation of mass, momentum, and energy in the liquid and in the vapor coupled by suitable interface conditions. It is, however, possible to considerably simplify the problem with the aid of reasonable approximations.

In the first place, the volume expansion coefficient of many refrigerants at their normal boiling point is typically small, of the order of $10^{-3}\,\mathrm{K}^{-1}$, e.g., $1.90 \times 10^{-3}\,\mathrm{K}^{-1}$ for ammonia at 239.75 K, $1.96 \times 10^{-3}\,\mathrm{K}^{-1}$ for refrigerant 12 at 243.2 K, and $0.750 \times 10^{-3}\,\mathrm{K}^{-1}$ for water at 373.15 K. Thus, with temperature oscillations of the order of a few degrees, thermal expansion is small and can be neglected. Second, the condition of conservation of mass across the liquid–vapor interface stipulates that

$$\dot{m} \equiv \rho_V(\dot{R}-v) = \rho_L(\dot{R}-u), \tag{1}$$

where $\dot{m}$ is the interfacial mass flux (positive for evaporation), ρ_V and ρ_L are the vapor and liquid densities, v and u the corresponding velocities, and $\dot{R}$ the velocity of the interface. This relation shows that the difference between the liquid and interface velocities is $\dot{m}/\rho_L$. For water, for example, even for heat fluxes as large as 1 MW/m², the mass flux is about 1 kg/m² s, which gives $|u-\dot{R}| \sim 10^{-3}$ m/s, that is completely negligible in comparison with typical values of $\dot{R}$ of the order of 1 m/s or greater. Hence, the approximation $u \simeq \dot{R}$ is completely reasonable.

These arguments show that, even in boiling conditions, the liquid motion can be handled in the same way as for the more familiar case of gas bubbles in a "cold" liquid. It is

well known that, in such a case, a good model for the radial dynamics of the bubble is furnished by the Keller equation[24–26]

$$\left(1-\frac{\dot{R}}{c}\right)R\ddot{R}+\frac{3}{2}\left(1-\frac{1}{3}\frac{\dot{R}}{c}\right)\dot{R}^2$$
$$=\frac{1}{\rho_L}\left(1+\frac{\dot{R}}{c}+\frac{R}{c}\frac{d}{dt}\right)[p_B-P(t)]+O(c^{-2}). \qquad (2)$$

In this equation dots denote time derivatives, c is the speed of sound in the liquid, $P=P(t)$ denotes the sum of the static ambient pressure and the time-dependent pressure field driving the bubble into oscillation, and p_B is the pressure on the liquid side of the interface, related to the bubble internal pressure p by the balance of normal stresses across the interface, namely

$$p=p_B+\frac{2\sigma}{R}+4\mu\frac{\dot{R}}{R}, \qquad (3)$$

in which σ is the surface tension coefficient and μ the liquid viscosity. In the present study we consider ambient pressures of the form

$$P(t)=p_\infty-P_A\sin\omega t, \qquad (4)$$

where p_∞ is the static pressure, P_A the acoustic pressure amplitude, and ω the sound angular frequency.

While we include liquid compressibility effects in the radial equation (2) to account for energy losses by acoustic radiation, we can neglect such effects in the liquid energy equation in view of the fact that, in any case, the liquid temperature field is affected by the bubble only over regions that are much smaller than the wavelength of sound. We thus write

$$\frac{\partial T_L}{\partial t}+\frac{R^2\dot{R}}{r^2}\frac{\partial T_L}{\partial r}=\frac{D_L}{r^2}\frac{\partial}{\partial r}\left(r^2\frac{\partial T_L}{\partial r}\right), \qquad (5)$$

where T_L is the liquid temperature, $(R^2/r^2)\dot{R}$ is the incompressible velocity field at a distance r from the bubble center, and D_L denotes the thermal diffusivity of the liquid. (Strictly speaking, we should write u in place of $\dot{R}$ in this equation, but the difference is negligible.)

A standard simplification in the dynamics of gas bubbles in sound fields of moderate amplitude is to treat the bubble internal pressure as spatially uniform.[27] This approximation, which hinges on the smallness of the Mach number of the vapor flow, holds also in the case of vapor bubbles, and actually even more so in view of the fact that the acoustic pressures of interest are usually smaller than in acoustic cavitation. It can be shown that, from this approximation and from the assumption of perfect-gas behavior of the vapor, one can derive the following expression for the vapor velocity:[27–30]

$$v=\frac{1}{\gamma p}\left[(\gamma-1)k_V\frac{\partial T_V}{\partial r}-\frac{1}{3}r\dot{p}\right], \qquad (6)$$

where γ is the ratio of the specific heats and k_V the thermal conductivity. The unknown vapor temperature field can then be found from the energy equation in the form

$$\rho_V c_{pV}\left(\frac{\partial T_V}{\partial t}+v\frac{\partial T_V}{\partial r}\right)-\dot{p}=\frac{1}{r^2}\frac{\partial}{\partial r}\left(k_V r^2\frac{\partial T_V}{\partial r}\right), \qquad (7)$$

where c_{pV} is the vapor specific heat at constant pressure.

The conservation of energy at the interface requires that

$$k_L\frac{\partial T_L}{\partial r}\bigg|_{r=R}-k_V\frac{\partial T_V}{\partial r}\bigg|_{r=R}=L\dot{m}, \qquad (8)$$

where L is the latent heat. Upon expressing $\dot{m}$ by means of (1) and v by (6), this relation gives

$$k_L\frac{\partial T_L}{\partial r}\bigg|_{r=R}=L\rho_V R\left(\frac{\dot{R}}{R}+\frac{\dot{p}}{3\gamma p}\right)+\frac{c_s}{c_{pV}}k_V\frac{\partial T_V}{\partial r}\bigg|_{r=R}, \qquad (9)$$

where

$$c_s=c_{pV}-\frac{L}{T_s} \qquad (10)$$

is the specific heat along the saturation line. For water at $100\,°C$, $c_s/c_{pV}\simeq-1.45$.

Due to kinetic effects, strict thermodynamic equilibrium does not prevail at an interface during phase change (see, e.g., Ref. 31). When the accommodation coefficient is not too small, these effects become appreciable only when the vapor Mach number approaches 1, which is far from the conditions that may reasonably be expected in the problem considered here. Such effects can also be important at frequencies high enough to be comparable with the inverse time for molecular relaxation. According to Gumerov,[32,33] the condition for the validity of thermodynamic equilibrium is

$$\frac{4\pi(\gamma-1)k_V T\omega}{\beta^2\gamma\rho_V L^2}\ll1, \qquad (11)$$

where β is the accommodation coefficient. Even for β as small as 0.04, at 1 kHz the value of this quantity is of the order of 10^{-5}, which shows that thermodynamic nonequilibrium effects are negligible.

On the basis of these considerations, we take the liquid and vapor temperature at the interface to have the same value T_S, and the vapor pressure to be given by the saturation relation

$$p=p_{sat}(T_S), \qquad (12)$$

with its derivative along the saturation line expressed by the Clausius–Clapeyron relation

$$\frac{dp}{dT_s}\bigg|_{sat}=\frac{L\rho_V}{T_s}. \qquad (13)$$

In view of the approximation of spatially uniform pressure, (12) gives the pressure everywhere in the bubble once the surface temperature is known. The local value of the temperature, however, varies from place to place according to the energy equation (7). The local value of the vapor density is given by the perfect-gas equation of state,

$$\rho_V = \frac{\gamma}{\gamma - 1} \frac{p}{c_{pV} T_V}. \tag{14}$$

III. LINEAR THEORY

In order to better appreciate the numerical results described in the next section it is useful to begin by a brief consideration of the linearized theory. Several versions of this theory, with a varying degree of complexity, have already been developed in the literature[34–36] and an abbreviated treatment will be sufficient.

It is postulated that the bubble can be dynamically stabilized around an average radius R_e to be determined. For linear oscillations, from the normal stress condition (3) it is clear that this is only possible provided that

$$p_0 = p_\infty + \frac{2\sigma}{R_e}, \tag{15}$$

where p_∞ is the static pressure and p_0 the mean pressure in the bubble. Under the action of the sound field, there is a net transport of heat into the bubble that causes a temperature rise and a consequent diffusive heat flux out of the bubble. A steady regime is reached when the two fluxes balance each other. In this dynamically stabilized state the mean bubble surface temperature T_{S0} is the saturation temperature corresponding to p_0 and is higher than the undisturbed liquid temperature T_∞. Furthermore, the liquid static pressure is also allowed to differ from saturation, and one writes

$$p_\infty = p_{\text{sat}}(T_\infty) + \Delta p. \tag{16}$$

The linearization follows the standard procedure. One sets

$$P = p_\infty + P_A \exp(i\omega t), \quad R = R_e + \Delta R \exp(i\omega t),$$

$$p = p_0 + \Delta p_V \exp(i\omega t), \tag{17}$$

$$T_S = T_{S0} + \Delta T_S \exp(i\omega t), \quad T_V = T_{S0} + \Delta T_V(r)\exp(i\omega t), \tag{18}$$

where Δ identifies the perturbation of the corresponding variable. The surface temperature perturbation ΔT_S is related to Δp_V as dictated by the saturation condition. The temperature field in the liquid is written as

$$T_L = T_\infty + \frac{R_e}{r}(T_{S0} - T_\infty) + \Delta T_L(r)\exp(i\omega t). \tag{19}$$

A consistent linearization of the mathematical model leads then to a system of linear equations that is readily solved. In particular,

$$\frac{\Delta R}{P_A} = \frac{1}{\rho_L R_e} \frac{-i}{\omega_0^2 + 2ib\omega - \omega^2}. \tag{20}$$

Here ω_0 and b play the formal role of natural frequency and damping parameter for the bubble oscillations and are given by

$$\omega_0^2 = \frac{1}{\rho_L R_e^2}\left(3\frac{K_r - B K_i}{K_r^2 + K_i^2} - \frac{2\sigma}{R_e} \right), \tag{21}$$
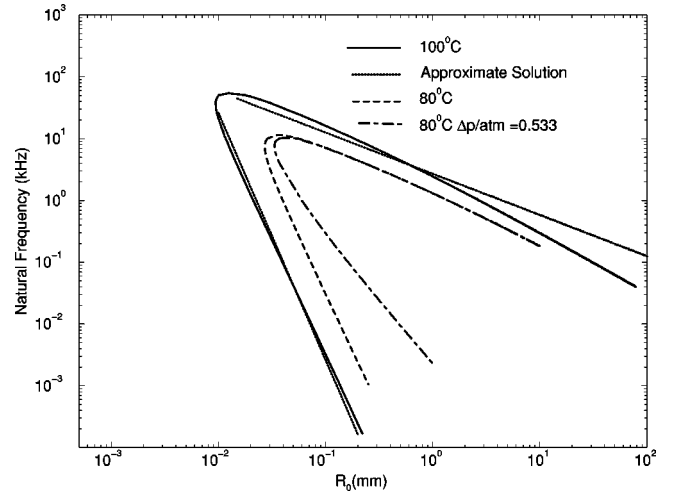

FIG. 1. The U-shaped lines portray the value of the frequency where the real part of the denominator of the radius perturbation amplitude (20) vanishes. —— $T_\infty = 100\,°C$, $p_\infty = p_{\text{sat}}(T_\infty)$; – – $T_\infty = 80\,°C$, $p_\infty = p_{\text{sat}}(T_\infty)$; ·–·· $T_\infty = 80\,°C$, $p_\infty = 1$ atm. The upper straight dashed line is the approximation (31) and the lower one the approximation (34).

$$b = \frac{3}{2\omega\rho_L R_e^2}\frac{K_i + B K_r}{K_r^2 + K_i^2}. \tag{22}$$

In these equations $K = -(1/V)dV/dp$, where V is the bubble volume, and can therefore be understood as the (complex) bubble compressibility; explicitly,

$$K \equiv K_r + iK_i = \frac{1}{\gamma p_0} + 3\frac{c_s}{L}\left(\frac{\gamma - 1}{\gamma}\frac{T_{S0}}{p_0} - \frac{dT_s}{dp} \right)$$

$$\times \left[\frac{D_V}{i\omega R_e^2} - \sqrt{\frac{D_V}{i\omega R_e^2}}\coth\left(\sqrt{\frac{i\omega R_e^2}{D_V}} \right) \right]$$

$$- \frac{3ik_L}{\rho_V L\omega R_e^2}\left(1 + \sqrt{\frac{iR_e^2\omega}{D_L}} \right)\frac{dT_s}{dp}, \tag{23}$$

while

$$B = 2\frac{k_L}{\rho_V L D_L}\frac{dT_s}{dp}\left(\Delta p + \frac{2\sigma}{R_e} \right)\left[1 - 3F\left(\sqrt{\frac{R_e^2\omega}{2D_L}} \right) \right]\frac{2D_L}{R_e^2\omega}, \tag{24}$$

with

$$F(x) = x^4\int_0^\infty \frac{\exp[-(1+i)t]}{(x+t)^5}dt. \tag{25}$$

In (23) D_V is the vapor thermal diffusivity. When the bubble is small compared with the thermal penetration depth in the gas, these expressions reduce to those of Alekseev.[34]

Over a broad parameter range, for a fixed sound frequency ω, a graph of ΔR vs R_e shows two peaks, which suggests the presence of two distinct resonant radii R_r and R_u for a vapor bubble.[17,18] It will be shown below that the smaller one of the two radii does not actually correspond to a true resonance but is unstable. Alternatively, setting to zero the real part of the denominator of (20), one finds two values of ω for each value of the radius. A typical example of such results is shown in Fig. 1 for the case of water. Here the solid

line is for $T_\infty = 100\,°C$ $\Delta p = 0$, the dashed line for $T_\infty = 80\,°C$ $\Delta p = 0$, and the dash-and-dot line for $T_\infty = 80\,°C$, $\Delta p/p_\infty = 0.533$, which is equivalent to $p_\infty = 1$ atm. The curves have two branches, the upper one of which corresponds to R_r and the lower one to R_u. The two branches join at a value of the radius below which no resonance exists.

At first sight it might appear surprising that a bubble containing only vapor exhibits any stiffness at all, let alone two distinct resonances. The key to these phenomena is to be found in the temperature dependence of the saturation pressure. More specifically, consider a vapor bubble the radius R_e of which decreases by an amount ΔR. This tends to cause the condensation of an amount of vapor

$$\Delta m_V = 4\pi R_e^2 \rho_V \Delta R. \tag{26}$$

If the process occurs with a frequency ω, the latent heat $L\Delta m_V$ liberated by the condensation increases the temperature of a shell of liquid of thickness $\sim \sqrt{D_L/\omega}$ by an amount

$$4\pi R_e^2 \sqrt{\frac{D_L}{\omega}} \rho_L c_L \Delta T_S = L\Delta m_V, \tag{27}$$

with c_L the liquid specific heat. This heating of the bubble surface increases the saturation pressure by an amount $\Delta p_V = (dp/dT_s)\Delta T_S$, where the derivative is taken along the saturation line. A force tending to resist compression is generated in this way,

$$F = 4\pi R_e^2 \Delta p_V \equiv -\mathcal{K}\Delta R, \tag{28}$$

where the following expression for a ''stiffness parameter'' $\mathcal{K}$ follows from the previous argument:

$$\mathcal{K} = 4\pi R_e^2 \sqrt{\frac{\omega}{D_L}} \frac{L\rho_V}{c_L\rho_L} \frac{dp_V}{dT_s} = 4\pi R_e^2 \sqrt{\frac{\omega}{D_L}} \frac{(L\rho_V)^2}{c_L\rho_L T_\infty}. \tag{29}$$

The Clausius–Clapeyron relation (13) has been used in the second step. The added mass for a sphere in radial motion is given by $\mathcal{M} = 4\pi R_e^3 \rho_L$, and therefore (29) enables one to estimate the resonance frequency ω_0 of the vapor bubble by $\omega_0^2 = \mathcal{K}/\mathcal{M}$ or

$$\omega_0^2 = \sqrt{\frac{\omega}{D_L}} \frac{(L\rho_V)^2}{R_e c_L T_\infty \rho_L^2}. \tag{30}$$

If $\omega \neq \omega_0$, this relation gives the position of the pole of the response function of $\Delta R(t)$ when the bubble is driven at frequency ω. By setting $\omega = \omega_0$, on the other hand, we find the natural frequency of the bubble as

$$\omega_0^3 R_r^2 \simeq \Theta_1 \frac{L^4 \rho_V^4}{\rho_L^3 c_L T_\infty^2 k_L}, \tag{31}$$

where k_L is the liquid thermal conductivity and a numerical constant Θ_1 has been introduced to account for the approximate nature of the derivation. With the value $\Theta_1 = 0.56$, the previous argument gives the upper dotted straight line in Fig. 2, which is seen to be in close agreement with the exact result. For comparison, it may be recalled that the natural frequency of a gas bubble in adiabatic oscillation at a pressure p_∞, with the neglect of surface tension, is given by
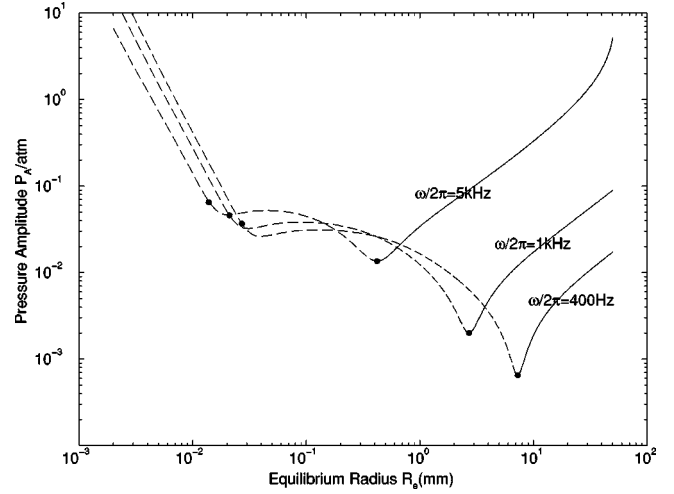

FIG. 2. Relation between the normalized pressure amplitude and the maximum radius R_e according to the quasilinear theory of Ref. 34, Eq. (35), at three different frequencies. The dots mark the resonant radii of Fig. 1. The dashed portions of the lines are unstable, the solid ones stable. The liquid is saturated water at 1 atm.

$$\omega_0^2 R_r^2 = \frac{3\gamma p_\infty}{\rho_L}. \tag{32}$$

This expression—and in particular its dependence on the bubble size—is very different from (31).

The second, lower resonance may be understood as follows. At low frequency, inertia and damping are small and can be ignored. The main effects are the restoring force previously described and the surface tension force

$$4\pi R_e^2 \Delta\left(\frac{2\sigma}{R}\right) \equiv -\mathcal{K}_\sigma \Delta R. \tag{33}$$

These two forces tend to oppose each other and, in suitable conditions, can balance. This circumstance leads to an oscillating system forced by the sound field, but with a negligibly small restoring force. The oscillation amplitude is then large, which superficially looks like a second resonance. Proceeding as before, equating (28) and (33), and again adjusting a numerical constant, we find

$$\omega_0 R_u^4 = \Theta_2 D_L \left(\frac{2\sigma c_L \rho_L T_\infty}{(L\rho_V)^2}\right)^2. \tag{34}$$

This result is shown by the lower straight dotted line in Fig. 1 for $\Theta_2 = 0.94$; again there is a fairly good agreement with the exact one. This physical argument also shows, however, the true nature of this second ''pseudoresonance.'' Indeed, if the bubble radius is smaller than this ''resonant'' value, the surface tension effect is so large as to give rise to a negative stiffness and the bubble will collapse unstably. Conversely, it will grow for a bigger value of the radius.

So far the equilibrium radius R_e is an arbitrary parameter, given which the preceding formulas determine resonance frequency, pressure amplitude, etc. As shown by Alekseev,[34] the linear theory can be extended to a weakly nonlinear one capable of determining a value of R_e for a given acoustic pressure amplitude P_A. The result of this analysis is (see also Refs. 35,36)

$$\left(\frac{2}{3}K_r - \frac{c_s R_e (dT_s/dp)}{2L\sqrt{2D_L/\omega}} - \frac{d^2 T_s/dp^2}{4dT_s/dp} - \frac{1}{36}\rho_L \omega^2 R_e^2 |K|^2 \right) P_A^2$$

$$= \left| 1 - \frac{1}{3}K\left(\frac{2\sigma}{R_e} + \rho_L \omega^2 R_e^2 \right) \right|^2 \left(\Delta p + \frac{2\sigma}{R_e} \right). \tag{35}$$

A graph of this curve, again for the case of water at 100 °C with $\Delta p = 0$, is shown in Fig. 2 for several acoustic frequencies. For each frequency, the two resonant values of the radius of Fig. 1 are marked by dots. Equation (35) has been improved by Gumerov,[33] whose results, however, are very close for the cases considered here. [In Fig. 2 the slight shift of R_u from the local minimum is due to the fact that the peak of ΔR given by (20) does not exactly coincide with the vanishing of the real part of the denominator, which is the condition used to calculate R_u.] The portion of the curve to the left of the larger resonance radius R_r is dashed and corresponds to a condition of unstable equilibrium, while the portion to the right is predicted to be stable. Notice that the derivation of the result (35) requires the assumption that the temperature field in the neighborhood of the bubble has stabilized to steady periodic conditions.

In summary, the key predictions of the linear theory that will be examined numerically in the light of the fully nonlinear model of Sec. II are: (a) the existence of a resonant radius; (b) the existence, at a given pressure amplitude, of a smallest value of the radius below which the bubble cannot be dynamically stabilized; (c) the existence, at a given pressure amplitude, of a largest value of the radius that functions as an attractor for bubbles with different initial radii.

IV. NUMERICAL RESULTS

A numerical solution of the system of equations described in Sec. II has been obtained by means of a spectral approximation to the temperature fields in the vapor and in the liquid. We have found that the numerical treatment of the problem is quite delicate and the results are sensitive even to comparatively small errors. Details of the method and of the validation of the code are provided in the Appendix. All the results shown here are for water.

Figure 3 shows the behavior of the bubble radius, normalized by the linear resonance radius $R_r = 2.71$ mm, as a function of time for $\omega/2\pi = 1$ kHz, $P_A = 0.4$ atm. The liquid is water at $T_\infty = 100$ °C and $p_\infty = 1$ atm, so that $\Delta p = 0$. The initial value of the radius is 35 μm, which is slightly larger than the linear pseudoresonant radius R_u that equals 21 μm in this case. It is seen that the bubble starts growing immediately due to the phenomenon of rectified heat transfer[19] and develops a distinct nonlinear response first with a weak third harmonic and then a prominent second harmonic during the first few cycles. The resonant radii at three and two times the driving frequency are 0.913 and 1.26 mm, which correspond to normalized values of 0.34 and 0.46. These harmonic components therefore develop as a nonlinear effect much as in the case of gas bubbles.[37,38] Most likely a similar nonlinear behavior is responsible for the subharmonic emissions observed by Neppiras and Finch,[4] in their study of acoustic cavitation in cryogenic liquids. When the mean radius ap-
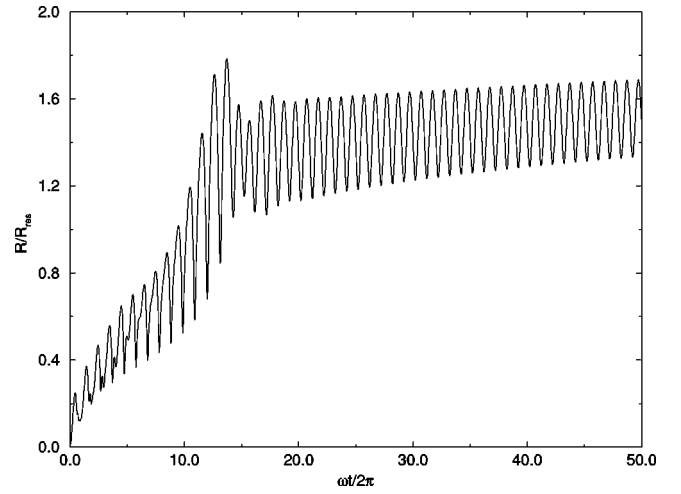
FIG. 3. Bubble radius (normalized by the linear resonant radius $R_r = 2.71$ mm) versus time for saturated water at 1 atm. The sound amplitude is 0.4 atm and the frequency 1 kHz.

proaches the resonant value R_r, the oscillation amplitude increases substantially and the growth rate of the bubble correspondingly accelerates. Above this phase of rapid growth, the growth rate changes markedly to a very low value that keeps decreasing. Qualitatively similar results for liquid nitrogen and hydrogen have been published by Akulichev.[39] We have found the same behavior in all the cases we have investigated, some further examples of which are shown in Fig. 4 for the same conditions as Fig. 3 but with different values of P_A. In some cases we have continued the integration for several tens of thousands of cycles, always finding a decreasing growth rate that, although small, is definitely not zero. These results are at variance with the linear theory prediction of the existence of a limiting value for the radius. Further comments on this matter will be found in the next section.

Figure 5 shows the mass flux at the bubble interface (positive for evaporation) for the highest-amplitude case ($P_A = 0.8$ atm) of Fig. 4. The very large values of these fluxes are worthy of note. Even during the later period of
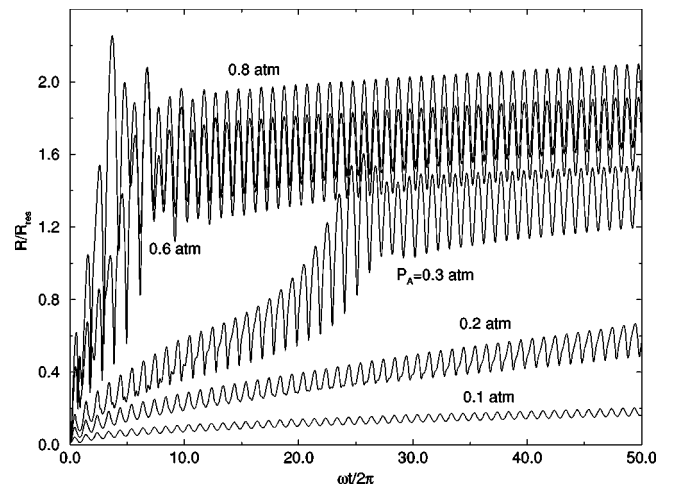
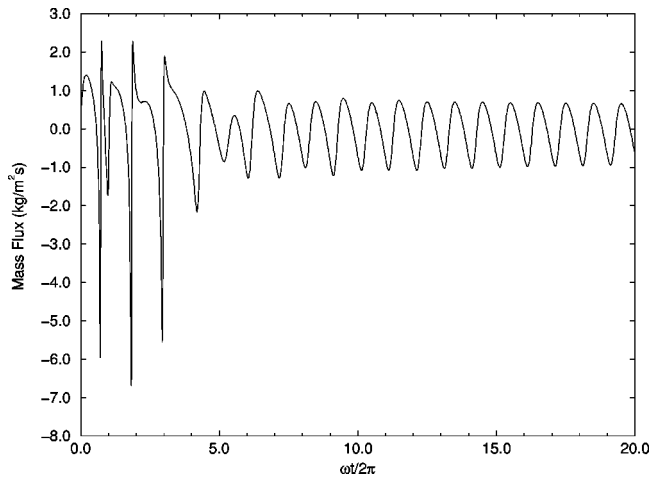FIG. 4. As in Fig. 3 for different acoustic pressure amplitudes P_A.

FIG. 5. Mass flux at the bubble wall (positive for evaporation) for the case in Fig. 4 with $P_A = 0.8$ atm.
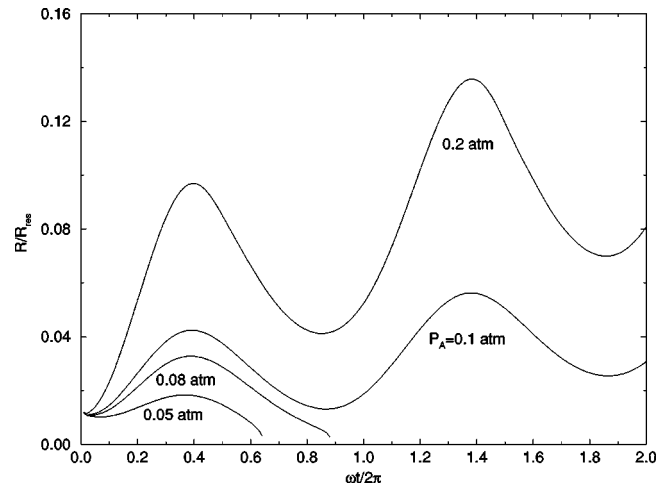

FIG. 6. Bubble behavior near the unstable region of Fig. 2 for saturated water at 1 atm and different acoustic pressure amplitudes. The initial bubble radius is 35 μm and the acoustic frequency 1 kHz.

slow growth and relatively small-amplitude oscillation, the mass flux is about 0.7 kg/m^2 s, which is equivalent to a heat flux of 1.5 MW/m^2.

If the integration is started from a radius near limit value of linear theory, the bubble is found to first shrink and then slowly turn around and start growing. This behavior can be explained by the fact that the evolution of the temperature field in the neighborhood of the bubble takes a large number of cycles but, once a quasisteady temperature distribution has been attained, growth sets in. The nonoscillatory component of the temperature field [cf. the second term in the right-hand side of (19)] is significant over a distance of order R from the bubble, and the time required for a temperature perturbation to reach this distance is of the order of R^2/D_L. The total number of cycles needed is therefore of the order of $\omega R^2/2\pi D_L$. For $\omega/2\pi \sim 1$ kHz, $R \sim 1$ mm, this is of the order of 10 000, which is in agreement with the numerical evidence. This extremely long development time of the temperature distribution in the neighborhood of the bubble is a significant difficulty in the computational study of these phenomena not only in terms of computer resources but, more significantly, of accuracy requirements.

In view of the slow development of the temperature field, it is also difficult to study the bubble behavior in the neighborhood of the unstable value R_u predicted by the linear theory and shown by the lower branch of the lines in Fig. 1. Ideally, it would be necessary to start the calculation with an already fully developed temperature field, which is clearly not feasible. Some typical results obtained with the initial condition $T_L = T_\infty$ are shown in Fig. 6 for the same conditions as in Figs. 3 and 4. The frequency is 1 kHz and the initial radius 35 μm which, according to the result shown in Fig. 2, would require an acoustic pressure in excess of 0.033 atm for bubble growth. The numerical results show instead that, for values of P_A smaller than 0.1 atm, the radius tends to zero, implying a complete collapse of the bubble. The difference between this value and the linear theory prediction is likely due to the different initial temperature distributions in the liquid. For $P_A \geqslant 0.1$ atm, however, the bubble starts growing immediately. Qualitatively the result is therefore as

predicted, although it is found that the outcome of the process is also sensitive to the phase of the pressure field at the start of the calculation. If the initial phase is one of compression (which can be simulated by using a negative value for P_A), rather than expansion, we find collapse even for $|P_A| > 0.1$, as shown in Fig. 7.

If the liquid is superheated, so that $\Delta p < 0$, the bubble will grow spontaneously provided the effect of surface tension is sufficiently weak. An interesting consequence of rectified heat transfer is the possibility to accelerate this growth. An example is shown in Fig. 8 where $\Delta p = -0.1$ atm, which corresponds to a water superheat of 2.3 K; the acoustic pressure amplitudes are 0, 0.2, and 0.4 atm. It is evident that there is a striking effect on the bubble growth rate, which might be useful to enhance boiling heat transfer in certain situations. The effect is, however, much less dramatic as the liquid superheat is increased, as Fig. 9 shows for $\Delta p = -0.2$ atm, which corresponds to a superheat of 4.8 K. The oscillating lines are for $P_A = 0.2$ and 0.5 atm.
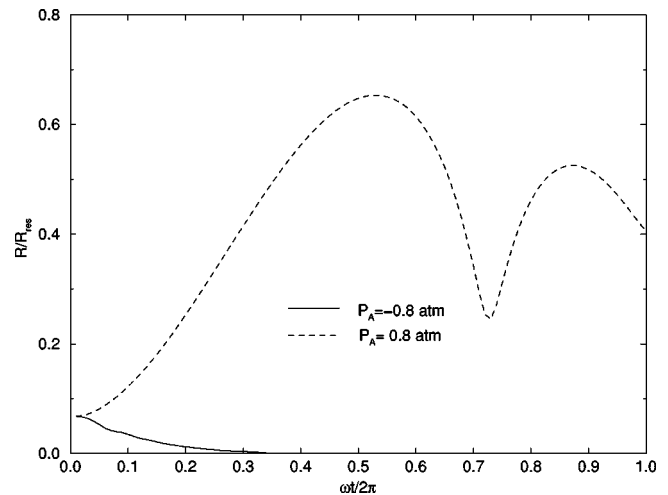

FIG. 7. Effect of the sound phase on the behavior of a bubble near the unstable region of Fig. 2 for $R(0) = 185$ μm; other conditions as in the previous figure. Solid line: $P_A = -0.8$ atm; dashed line $P_A = 0.8$ atm.
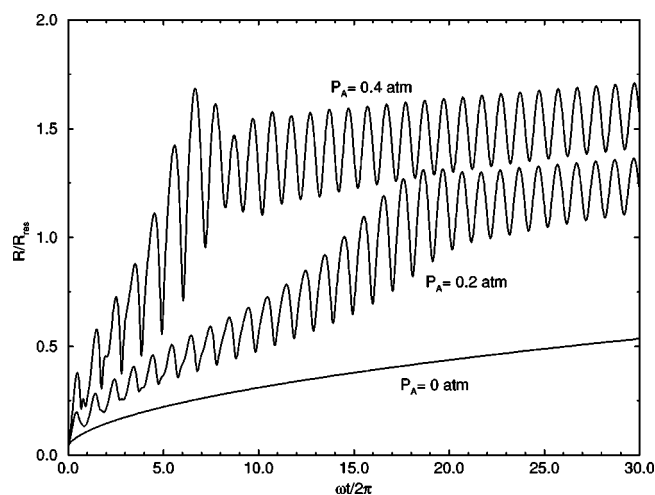
FIG. 8. Effect of a sound field on bubble growth in water at 1 atm with a 2.3 K superheat at 1 kHz. The three lines are, in ascending order, for $P_A = 0$, 0.2, and 0.4 atm. The initial bubble radius is 100 μm and $R_r = 2.71$ mm.

It is well known that gas bubbles driven by a sufficiently large acoustic pressure exhibit chaotic behavior.[40,41] We have not encountered any trace of such behavior for the vapor bubbles studied in this paper. Only if the interfacial energy balance relation (8) is approximated by (37), derived in the Sec. VI, does one encounter a chaotic response. It appears probable therefore that, with the full model, chaos could be found at a stronger forcing, although the assumption of sphericity would most likely be inapplicable in these conditions.

V. LIMITING RADIUS

As mentioned in the previous section, our results are incompatible with the linear-theory prediction of a limiting value of the radius. Very recently, Gumerov[42] has considerably extended the analytical theory by using a multiple-time-scale approach coupled with a singular-perturbation treatment of the temperature field near the bubble. He finds that,
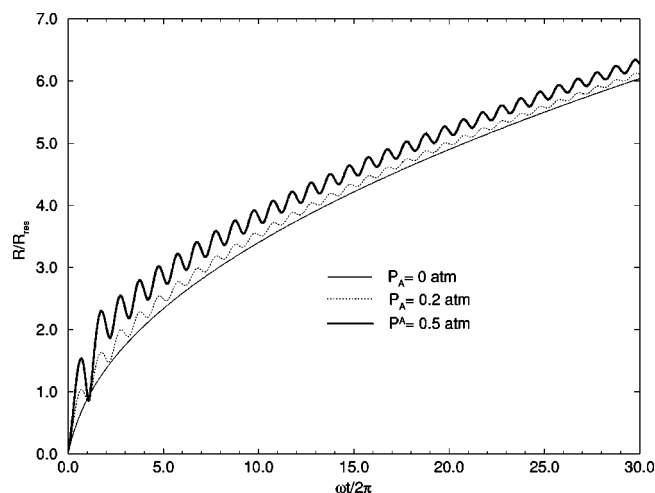
up to a certain order of accuracy in the acoustic pressure amplitude, the average growth rate of the bubble equals a certain expression. By equating this expression to zero, he predicts a limiting value of the radius in qualitative agreement with the linear theory result. From his analysis, however, it is not possible to determine what would be the effect of keeping more and more terms in the expansion. It could be that the limiting value of the radius would increase at each order of the perturbation calculation, which would essentially confirm our results.

In the conventional linear theory it is assumed that the liquid temperature near the bubble has reached a quasisteady distribution. This assumption is strictly correct only at threshold conditions, where the net heat flux into the bubble vanishes. In reality, as the average bubble radius grows or shrinks, there is a slowly evolving average temperature field superimposed on the oscillatory temperature distribution. It could be that failure to account for this feature is responsible for the result of a limiting value of the radius in the linear theory. This effect is included (approximately) in Gumerov's analysis but it does not change the final prediction.

We have validated our calculations by repeating them many times with different values of the numerical parameters such as the number of terms retained in the spectral expansion, error tolerance, etc., always with the same results. We are thus confident that this prediction is not a numerical artifact, at least up to several hundred cycles. Gumerov[43] has independently confirmed our calculations by a different numerical method. He estimates that the problem might lie in the fact that reaching the limiting radius might require several hundred thousand or even millions of cycles.[43] If so, a fully numerical investigation of the matter would place extreme demands on both computing resources and numerical accuracy and is clearly not feasible with our techniques.

Unfortunately, one cannot turn to experiment to resolve the question. The scant available experimental evidence is ambiguous and the accuracy with which experimental parameters—in particular the sound pressure amplitude at the location of the bubble—are known not very good (in this connection see comments in Ref. 44). Marston[45] studied vapor bubbles in He II at 2.09 K and found a continuous growth until the bubbles became unstable and broke up. In a later experiment with He I at 4.2 K, Marston and Greene[20] observed circular arcs of seemingly stable vapor bubbles. We have tried to reproduce these results but have encountered the fundamental difficulty that the predicted surface temperature of a He I bubble exceeds the critical point during the compression phase of the oscillations. In view of its very large thermal conductivity, a bubble in He II has essentially no stiffness. In both cases, therefore, the physical situation is quite different from that of ordinary liquids studied in this paper.

For a liquid like water in ordinary conditions at frequencies in the kHz range, the practical consequences of this unresolved point are minor as the predicted limit radius is unrealistically large (tens of centimeters) and therefore outside the range of practical interest. For other liquids, or at higher frequencies, however, the situation would be differ-

FIG. 9. As in Fig. 8 for a superheat of 4.8 K at 10 kHz. The initial radius is 10 μm and the resonant radius 0.17 mm. The pressure amplitudes are 0, 0.2, and 0.5 atm.

ent. Experiments directly addressing this matter would be of great interest.

VI. NEARLY ISOTHERMAL CASE

The model of Sec. II is somewhat complex and it is desirable to develop accurate simplifications of it. We consider here the case in which the bubble interior can be considered nearly isothermal. The most straightforward application of this idea can be based on the identity

$$4\pi R^2 \rho_V(\dot{R}-v) = \frac{d}{dt}\left(4\pi\int_0^R r^2\rho_V dr\right), \tag{36}$$

which is easily proven with the aid of the continuity equation. If it is assumed that the phase change at the bubble surface is dominated by the liquid-side heat transfer, and that the bubble density is spatially uniform, the interfacial energy condition (8) then gives

$$4\pi R^2 k_L \frac{\partial T_L}{\partial r}\bigg|_{r=R} = L\frac{d}{dt}\left(\frac{4}{3}\pi R^3 \rho_V\right), \tag{37}$$

an approximation that has been extensively used in the boiling literature (see, e.g., Ref. 46, Chs. 6 and 7).

In order to examine the validity of this expression and possibly extend it, it is useful to proceed formally on the assumption that the square of the ratio between the characteristic bubble radius and the thermal penetration length in the vapor

$$\epsilon = \frac{\omega R^2}{D_V}, \tag{38}$$

where D_V is the vapor thermal diffusivity, is small. The method is similar to that described in Ref. 27 for the case of a gas bubble.

Since we are not going to limit ourselves to small-amplitude motion of the bubble radius, it is convenient to immobilize the bubble surface by using the new coordinate

$$y = \frac{r}{R(t)}. \tag{39}$$

Furthermore, we make the energy equation (7) dimensionless by defining

$$t^* = \omega t \quad R^* = \frac{R}{R_0} \quad T^* = \frac{T_V}{T_\infty} \quad p^* = \frac{p}{p_0}, \tag{40}$$

where the index 0 denotes undisturbed values. The vapor energy equation then becomes

$$\frac{\partial T^*}{\partial t^*} - \left[\left(\frac{\gamma-1}{\gamma}\right)T^* + \frac{y}{3\gamma}\frac{\partial T^*}{\partial y}\right]\frac{p^{*\prime}}{p^*}$$

$$= \frac{T^*}{\epsilon p^* R^{*2}}\frac{1}{y^2}\frac{\partial}{\partial y}\left(y^2\frac{\partial T^*}{\partial y}\right) - \frac{1}{\epsilon p^* R^{*2}}\left(\frac{\partial T^*}{\partial y}\right)^2$$

$$+ \frac{R^{*\prime}}{R^*}y\frac{\partial T^*}{\partial y}, \tag{41}$$

where the apostrophe denotes differentiation with respect to the dimensionless time. We now seek a perturbation solution of (41) by expanding T^* in terms of the small parameter ϵ,

$$T^* = T_S^* + \epsilon T_1 + \epsilon^2 T_2 + \cdots. \tag{42}$$

Upon substituting into (41) and equating coefficients of like powers of ϵ we find, at the lowest order,

$$\frac{1}{y^2}\frac{\partial}{\partial y}\left(y^2\frac{\partial T_1}{\partial y}\right) = p^* R^{*2}\left(\frac{T_S^{*\prime}}{T_S^*} - \frac{\gamma-1}{\gamma}\frac{p^{*\prime}}{p^*}\right). \tag{43}$$

The solution regular at the origin and vanishing at the bubble surface is

$$T_1 = \frac{\alpha}{6}(y^2-1), \tag{44}$$

where, for convenience, we have defined

$$\alpha = p^* R^{*2}\left(\frac{T_S^{*\prime}}{T_S^*} - \frac{\gamma-1}{\gamma}\frac{p^{*\prime}}{p^*}\right). \tag{45}$$

Upon expressing T_1 in dimensional form and substituting into the condition (9) of energy conservation at the interface, we find

$$4\pi R^2 k_L \frac{\partial T_L}{\partial r}\bigg|_{r=R} = L\frac{d}{dt}\left(\frac{4}{3}\pi R^3 \rho_V\right) + \frac{4}{3}\pi R^3 \rho_V c_s\frac{dT_S}{dt}. \tag{46}$$

The first term in the right-hand side is identical to the right-hand side of the approximation (37). As for the second term, it can be expected to be small whenever the time derivative of T_S is. Since the bubble surface in ordinary boiling quickly attains the saturation value, the use of (37) is thus justified in these conditions. In the presence of forced bubble oscillations, however, the bubble surface temperature fluctuates at the same frequency as the forcing and it will be seen shortly that the second term in (46) is far from negligible in comparison with the first one.

A comparison of the approximation (46) with the results of the complete model of Sec. II in a few cases is presented in Figs. 10 to 13. Two values of ϵ are quoted, ϵ_r and ϵ_0, corresponding to the linear resonance radius R_r and the initial radius $R(0)$, respectively. Figures 10 and 11 are for a frequency of 400 Hz in saturated water at 1 atm, for pressure amplitudes of 0.5 and 0.8 atm, respectively. The initial radius is 35 μm and the corresponding value of ϵ, $\epsilon_0 = 0.021$. The value based on the (linear) resonance radius is instead $\epsilon_r = 902$. The result at the lower P_A shows some large discrepancies when the bubble reaches its resonance radius, which, however, quickly diminish in the phase of slow growth. A higher drive or a higher frequency (Figs. 12 and 13, for $\omega/2\pi = 5$ kHz, $\epsilon_0 = 0.26$, $\epsilon_r = 38$ and the same initial radius) both result in a smaller error. The good performance of the nearly isothermal approximation even when the parameter ϵ is not particularly small is remarkable. The zero-order approximation (37) is instead rather poor unless the frequency is exceedingly small, as shown for a typical case by the dotted line in Fig. 10.

Continuing with the perturbation procedure, to first order in ϵ we find an equation for T_2,
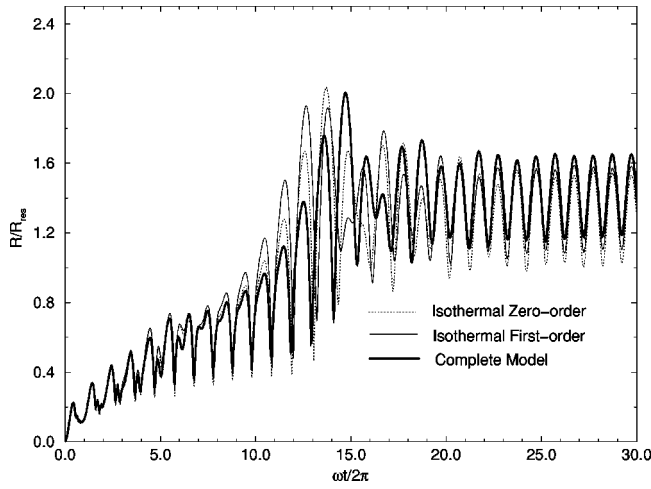
FIG. 10. Bubble growth according to the nearly isothermal approximation (46) (thin line) and the complete model of Sec. II (thick line) for saturated water at 1 atm with $\omega/2\pi = 400$ Hz and $P_A = 0.5$ atm. The dotted line is the zero-order approximation (37). The initial value of the radius is 35 μm and $R_r = 7.27$ mm.

FIG. 12. As in Fig. 10 with $\omega/2\pi = 5$ kHz and $P_A = 0.5$ atm. The initial value of the radius is 35 μm and $R_r = 0.42$ mm.

$$\frac{\partial}{\partial y}\left(y^2 \frac{\partial T_2}{\partial y}\right) = y^2 \frac{p^* R^{*2}}{T_S^*}\frac{\partial T_1}{\partial t^*} - \left(\frac{\gamma-1}{\gamma}T_1 + \frac{y}{3\gamma}\frac{\partial T_1}{\partial y}\right)$$
$$\times y^2 \frac{p^{*\prime} R^{*2}}{T_S^*} - \frac{T_1}{T_S^*}\frac{\partial}{\partial y}\left(y^2 \frac{\partial T_1}{\partial y}\right)$$
$$+ \frac{y^2}{T_S^*}\left(\frac{\partial T_1}{\partial y}\right)^2 - \frac{p^* R^* R^{*\prime}}{T_S^*}y^3 \frac{\partial T_1}{\partial y}. \quad (47)$$

After substitution of (44) for T_1, this equation is readily solved with the same boundary conditions as before, to find

$$T_2 = \frac{p^* R^{*2}}{12 T_S^*}\left\{ \frac{1}{10}\left[\alpha' - \frac{\alpha}{\gamma}\left(\gamma - \frac{1}{3}\right)\frac{p^{*\prime}}{p^*} - \frac{\alpha^2}{3 p^* R^{*2}}\right.\right.$$
$$\left. - 2\alpha \frac{R^{*\prime}}{R^*}\right](y^4 - 1) + \frac{1}{3}\left[\frac{\gamma-1}{\gamma}\alpha \frac{p^{*\prime}}{p^*} - \alpha'\right.$$
$$\left.\left. + \frac{\alpha^2}{p^* R^{*2}}\right](y^2 - 1)\right\}. \quad (48)$$

The interfacial energy conservation relation (9) now gives

$$k_L \frac{\partial T_L}{\partial r}\bigg|_{r=R} = L\rho_V \left(\dot{R} + \frac{R}{3}\frac{\dot{\rho}_V}{\rho_V}\right) + \frac{1}{3}R\rho_V c_s \frac{dT_S}{dt}$$
$$- \left(\frac{\gamma}{\gamma-1}\frac{c_s}{c_{pV}}\right)^2 \frac{R^3 p^2}{45 k_V T_S}\left[\frac{\ddot{T}_S}{T_S} + 5\frac{\dot{R}}{R}\frac{\dot{T}_S}{T_S}\right.$$
$$\left. + \left(\frac{L}{c_s T_S} + \frac{2\gamma}{\gamma-1}\frac{L}{c_{pV} T_S} - 3\right)\left(\frac{\dot{T}_S}{T_S}\right)^2\right]. \quad (49)$$

Unfortunately, this second-order result (49) is found numerically to be stable only in a relatively restricted parameter range, where it does not give results significantly different from those of the first-order model (46). A typical example is shown in Fig. 14.

VII. CONCLUSIONS

We have examined the spherical dynamics of a vapor bubble in an oscillating pressure field. One of our objectives was the examination of several predictions of linear theory,
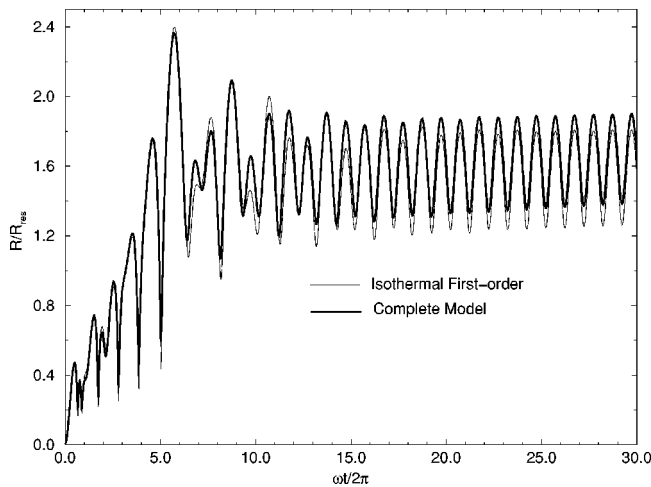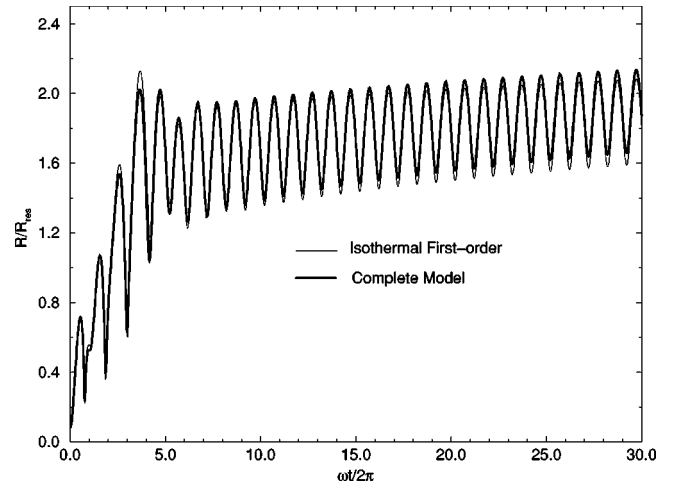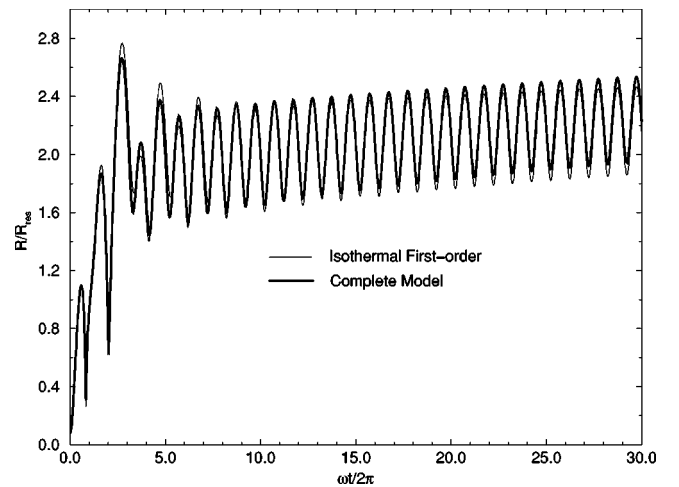

FIG. 11. As in the previous figure for $P_A = 0.8$ atm.

FIG. 13. As in Fig. 10 with $\omega/2\pi = 5$ kHz and $P_A = 0.8$ atm.

Phys. Fluids, Vol. 11, No. 8, August 1999

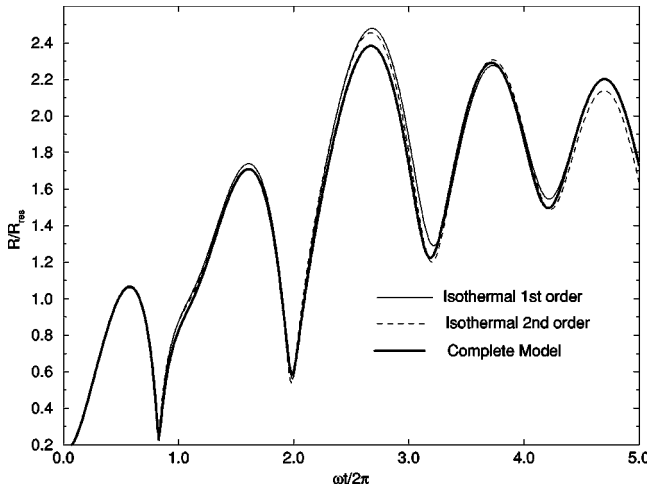Dynamics of vapor bubbles in acoustic pressure fields   2017

FIG. 14. Comparison of the first- and second-order nearly isothermal approximations [(46), thin solid line, (49), dashed line] and the complete model of Sec. II (thick solid line) for saturated water at 1 atm with $P_A = 0.5$ atm, $\omega/2\pi = 10$ kHz, and an initial radius of 30 μm. Here $R_r = 0.17$ mm.

such as the existence of two resonant radii and of a dynamically stable limit bubble size. The smaller resonant radius has been found to actually mark a stability limit for the bubble, and the numerical evidence argues against the existence of a limit bubble size. A significant obstacle in the study has been the slowness with which the temperature distribution develops in the host liquid compared with the oscillations induced by the pressure field. It would seem that recourse to experiment would be required to obtain more definite answers.

We have also obtained a simplification of the model valid when the thermal penetration length in the vapor is larger than the bubble radius, Eq. (46). The approximation proves useful over a rather broad range of parameters and, even where it is not precise, it preserves the qualitative features of the complete theory.

The insight gained in the course of this study suggests a broad range of possible interesting phenomena and applications. For example, a striking aspect of the bubble response of Figs. 3 and 4 is the rapidity of the growth below the resonance radius R_r and its slowness above R_r. This feature may have implications for the enhancement of boiling heat transfer by acoustical means.[9–13] It would seem that, by adjusting the frequency so that R_r is close to the size at which the bubbles detach from the heated surface, a faster growth/detachment bubble cycle can be induced with an attendant increase in heat transfer.

The continuous growth of the bubble in a saturated liquid, or even in a liquid colder than saturation, indicates the possibility of boiling heat transfer with exceedingly small—or negative—superheats.

The existence, for a given ambient pressure, of a smallest value of the radius below which the bubble is unstable suggests a mechanism by which shock waves in liquids containing vapor bubbles might be significantly amplified by causing the complete collapse of the bubbles.[6,8] This process could have implications for the propagation of vapor explosions (see, e.g., Ref. 47).

ACKNOWLEDGMENTS

APPENDIX: NUMERICAL METHOD

We give here a few details on the numerical methods and procedures used for code validation.

The energy equations in the vapor and in the liquid are solved by a spectral collocation method, the application of which requires that the boundaries of the integration domain be fixed. For this purpose, for the vapor region, we use the variable y defined in (39), in terms of which the vapor energy equation (7) becomes

$$\frac{\gamma}{\gamma-1}\frac{p}{T_V}\left\{\frac{\partial T_V}{\partial t} + \frac{1}{\gamma p R^2}\left[(\gamma-1)k_V\frac{\partial T_V}{\partial y} - \frac{1}{3}yR^2\dot{p}\right]\right.$$
$$\left.\times\frac{\partial T_V}{\partial y} - \frac{\dot{R}}{R}y\frac{\partial T_V}{\partial y}\right\} - \dot{p} = \frac{k_V}{R^2 y^2}\frac{\partial}{\partial y}\left(y^2\frac{\partial T_V}{\partial y}\right). \quad (A1)$$

We then write

$$T_V = \sum_{n=0}^{M} b_n(t)T_{2n}(y), \quad (A2)$$

where the T_n's are the Chebyshev polynomials. Only the even polynomials are used to ensure that $\partial T_V/\partial r$ vanish at the bubble center. For the liquid region we use the auxiliary variable

$$x = \frac{l}{l+r-R(t)}, \quad (A3)$$

where l is taken to be a multiple B of the thermal penetration length $\sqrt{D_L/\omega}$ in the liquid,

$$l = B\sqrt{\frac{D_L}{\omega}}. \quad (A4)$$

Clearly, $x=1$ at the bubble surface while $x=0$ at infinity. In terms of x, the liquid energy equation (5) is

$$\frac{\partial T_L}{\partial t} + \frac{x^2}{l}\dot{R}\left[1 - \frac{R^2}{(l/x+R-l)^2}\right]\frac{\partial T_L}{\partial x}$$
$$= \frac{D_L}{(l/x+R-l)^2}\frac{x^2}{l}\frac{\partial}{\partial x}\left[(l/x+R-l)^2\frac{x^2}{l}\frac{\partial T_L}{\partial x}\right]. \quad (A5)$$

The spectral approximation to T_L is taken to be

$$T_L = \sum_{n=0}^{N} a_n(t)T_{2n}(x), \quad (A6)$$

where again only even polynomials are used to ensure that $\partial T_L/\partial r = 0$ at infinity.

Upon substitution of (A2), (A6) into (A1), (A5), a system of $N+M-1$ coupled ordinary differential equations is obtained by evaluating the equations at the $M+N-1$ collocation points,

$$y_j = \cos\frac{\pi j}{2M}, \quad j=1,2...,M,$$

$$x_k = \cos\frac{\pi k}{2N}, \quad k=1,2,...,N-1. \tag{A7}$$

The three missing equations necessary to determine the $N+M+2$ unknowns b_n, $n=0,1,...M$, a_n, $n=0,1,...N$, are the continuity of temperature at $r=R(t)$ and the energy boundary condition (9) and the condition $T_L=T_\infty$ at infinity.

In the numerical implementation of the method just described, we typically take $M=16$, $N=32$, and $B=10$. Larger values of these parameters did not significantly affect the numerical results. From the definition (A3) it is clear that the parameter B controls the distribution of nodes in the liquid, with larger values of B giving a denser distribution of nodes near the bubble at the expense of a sparser distribution in the far field. We have found that the numerical results were insensitive to B provided it was kept in the range between 10 and 50.

In earlier work on gas bubbles we have established the accuracy of the computational procedure for the bubble interior.[41] For the exterior problem, in order to establish the suitability of the mapping (A3), to ensure that a sufficient number of terms was retained in the expansion, and to validate the code, we have tested the method on a simpler problem that admits an analytic solution. Consider the spherically symmetric conduction equation

$$\frac{\partial T}{\partial t} = \frac{1}{r^2}\frac{\partial}{\partial r}\left(r^2\frac{\partial T}{\partial r}\right), \tag{A8}$$

subject to the condition $T\to 0$ as $r\to\infty$ while, at $r=1$,

$$\frac{\partial T(1,t)}{\partial t} = \zeta\frac{\partial T(1,t)}{\partial r} + f(t), \tag{A9}$$

where ζ and $f(t)$ are given. This condition resembles the boundary condition (9) or its approximations (37), (46) of the present problem.

With the initial condition $T(r,0)=0$, the analytic solution of the problem is

$$T(r,t) = \frac{C}{r}\int_0^t \left\{ E\exp[E(r-1)+E^2\tau] \right.$$

$$\times\text{erfc}\left(\frac{r-1}{2\sqrt{\tau}}+E\sqrt{\tau}\right) - D\exp[D(r-1)+D^2\tau]$$

$$\left.\times\text{erfc}\left(\frac{r-1}{2\sqrt{\tau}}+D\sqrt{\tau}\right)\right\} f(t-\tau)d\tau, \tag{A10}$$

where

$$\Delta^2 = \zeta(\zeta-4), \quad C = \frac{\zeta+\Delta}{\zeta(4-\Delta-\zeta)},$$
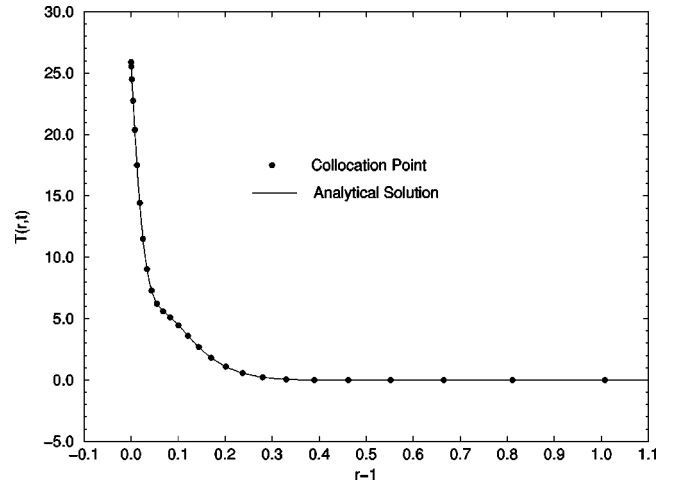

FIG. 15. The solid line shows the analytical solution of the model problem described in the Appendix. The dots mark the numerical solution and also the position of all but the last six collocation points.

$$D = \frac{1}{2}(\zeta+\Delta), \quad E = \frac{2\zeta}{\zeta+\Delta}.$$

To simulate the case of present concern we take $f = A\sin\omega t$. With this choice, recalling that

$$\int_0^t E e^{E^2\tau}\text{erfc}(E\sqrt{\tau})e^{i\omega(t-\tau)}d\tau$$

$$= \frac{E e^{i\omega t}}{E^2-i\omega}\left\{ e^{(E^2-i\omega)t}\text{erfc}(E\sqrt{t}) - 1 + \frac{E}{\sqrt{i\omega}}\text{erfc}(\sqrt{i\omega t})\right\},$$

a closed-form expression for $T(1,t)$ is readily found. For $r\neq 1$, the integral (A10) was calculated numerically.

The solid line in Fig. 15 shows the analytic solution (A10) for $\omega=3703$ s^{-1}, $\zeta=4.12$, $A=5880$ at $t=4.5/\omega$. The dots indicate the numerical result and, at the same time, the position of all but the last six of the collocation points used in the calculation.

[1] R. E. Apfel, ''Acoustic cavitation,'' in *Methods of Experimental Physics*, edited by P. D. Edmonds (Academic, New York, 1981), Vol. 19, pp. 355–411.

[2] T. G. Leighton, *The Acoustic Bubble* (Academic, London, 1994).

[3] Z. C. Feng and L. G. Leal, ''Nonlinear bubble dynamics,'' Annu. Rev. Fluid Mech. **29**, 201 (1997).

[4] E. A. Neppiras and R. D. Finch, ''Acoustic cavitation in helium, nitrogen and water at 10 kHz,'' J. Acoust. Soc. Am. **52**, 335 (1972).

[5] V. A. Akulichev, ''Acoustic cavitation in low-temperature liquids,'' Ultrasonics **24**, 8 (1986).

[6] R. I. Nigmatulin, N. S. Khabeev, and Z. N. Hai, ''Waves in liquids with vapour bubbles,'' J. Fluid Mech. **186**, 85 (1988).

[7] R. I. Nigmatulin, *Dynamics of Multiphase Media* (Hemisphere, Washington, 1991).

[8] V. E. Nakoryakov, B. G. Pokusaev, and I. R. Shreiber, *Wave Propagation in Gas-Liquid Media* (CRC, Boca Raton, 1993).

[9] K. A. Park and A. E. Bergles, ''Ultrasonic enhancement of saturated and subcooled pool boiling,'' Int. J. Heat Mass Transf. **31**, 664 (1988).

[10] A. Serizawa, M. Mukai, N. Aoki, O. Takahashi, Z. Kawara, K. Mishima, and I. Michiyoshi, ''Effect of ultrasonic emission on boiling and nonboiling heat transfer in natural and forced circulation systems,'' in *Proceedings of the X International Heat Transfer Conference*, Paper No. HA17, 1994, pp. 97–102.

[11] G. P. Celata, M. Cumo, and T. Setaro, ''Pressure wave perturbations effect on subcooled flow boiling of well-wetting fluids,'' in *Multiphase Flow*

Kyoto '95, edited by A. Serizawa, T. Fukano, and J. Bataille (Japan Society of Multiphase Flow, 1995), Vol. 2, pp. PC2-7–PC2-12.

[12] J. S. Sitter, T. J. Snyder, J. N. Chung, and P. L. Marston, ''Acoustic field interaction with a boiling system under terrestrial gravity and microgravity,'' J. Acoust. Soc. Am. **104**, 2561 (1998).

[13] J. S. Sitter, T. J. Snyder, J. N. Chung, and P. L. Marston, ''Terrestrial and microgravity pool boiling heat transfer from a wire in an acoustic field,'' Int. J. Heat Mass Transf. **41**, 2143 (1998).

[14] A. Prosperetti and H. N. Oğuz, ''Acoustic behavior of vapor bubbles,'' in *Proceedings of the 3rd Microgravity Fluid Physics Conference*, 1996, NASA.

[15] M. Zell, J. Straub, and B. Vogel, ''Pool boiling under microgravity,'' PCH, PhysicoChem. Hydrodyn. **11**, 813 (1989).

[16] J. Straub, ''Interfacial heat transfer and multiphase flow in microgravity,'' in *Multiphase Flow Kyoto '95*, edited by A. Serizawa, T. Fukano, and J. Bataille (Japan Society of Multiphase Flow, 1995), Vol. 2, pp. PL4-1–P114-12.

[17] R. D. Finch and E. A. Neppiras, ''Vapor bubble dynamics,'' J. Acoust. Soc. Am. **53**, 1402 (1973).

[18] T. Wang, ''Rectified heat transfer,'' J. Acoust. Soc. Am. **56**, 1131 (1974).

[19] T. Wang, ''Effects of evaporation and diffusion on an oscillating bubble,'' Phys. Fluids **17**, 1121 (1974).

[20] P. L. Marston and D. B. Greene, ''Stable microscopic bubbles in helium I and evaporation-condensation resonance,'' J. Acoust. Soc. Am. **64**, 319 (1978).

[21] P. L. Marston, ''Evaporation-condensation resonance frequency of oscillating vapor bubbles,'' J. Acoust. Soc. Am. **66**, 1516 (1979).

[22] N. S. Khabeev, ''Heat transfer and phase-transition effects in the oscillation of vapor bubbles,'' Sov. Phys. Acoust. **21**, 501 (1976).

[23] F. B. Nagiev and N. S. Khabeev, ''Heat-transfer and phase-transition effects associated with oscillations of vapor-gas bubbles,'' Sov. Phys. Acoust. **25**, 148 (1979).

[24] J. B. Keller and I. I. Kolodner, ''Damping of underwater explosion bubble oscillations,'' J. Appl. Phys. **27**, 1152 (1956).

[25] J. B. Keller and M. J. Miksis, ''Bubble oscillations of large amplitude,'' J. Acoust. Soc. Am. **68**, 628 (1980).

[26] A. Prosperetti and A. Lezzi, ''Bubble dynamics in a compressible liquid. Part 1. First-order theory,'' J. Fluid Mech. **185**, 289 (1986).

[27] A. Prosperetti, ''The thermal behaviour of oscillating gas bubbles,'' J. Fluid Mech. **222**, 587 (1991).

[28] R. I. Nigmatulin and N. S. Khabeev, ''Dynamics of vapor bubbles,'' Fluid Dyn. (USSR) **10**, 415 (1975).

[29] R. I. Nigmatulin, N. S. Khabeev, and F. B. Nagiev, ''Dynamics, heat, and mass transfer of vapour-gas bubbles in a liquid,'' Int. J. Heat Mass Transf. **24**, 1033 (1981).

[30] A. Prosperetti, L. A. Crum, and K. W. Commander, ''Nonlinear bubble dynamics,'' J. Acoust. Soc. Am. **83**, 502 (1988).

[31] D. A. Labuntsov and A. P. Kryukov, ''Analysis of intensive evaporation and condensation,'' Int. J. Heat Mass Transf. **22**, 989 (1979).

[32] N. A. Gumerov, ''The weak non-linear fluctuations in the radius of a condensed drop in an acoustic field,'' J. Appl. Math. Mech. (PMM U.S.S.R.) **53**, 203 (1989).

[33] N. A. Gumerov, ''Weakly non-linear oscillations of the radius of a vapour bubble in an acoustic field,'' J. Appl. Math. Mech. (PMM U.S.S.R.) **55**, 205 (1991).

[34] V. N. Alekseev, ''Steady-state behavior of a vapor bubble in an ultrasonic field,'' Sov. Phys. Acoust. **21**, 311 (1976).

[35] V. N. Alekseev, ''Nonsteady behavior of a vapor bubble in an ultrasonic field,'' Sov. Phys. Acoust. **22**, 104 (1976).

[36] V. A. Akulichev, V. N. Alekseev, and V. P. Yushin, ''Growth of vapor bubbles in an ultrasonic field,'' Sov. Phys. Acoust. **25**, 453 (1979).

[37] W. Lauterborn, ''Investigations of nonlinear oscillations of gas bubbles in liquids,'' J. Acoust. Soc. Am. **59**, 283 (1976).

[38] A. Prosperetti, ''Nonlinear oscillations of gas bubbles in liquids: Steady state solutions,'' J. Acoust. Soc. Am. **56**, 878 (1974).

[39] V. A. Akulichev, ''Acoustic cavitation in cryogenic and boiling liquids,'' Appl. Sci. Res. **38**, 55 (1982).

[40] U. Parlitz, V. Englisch, C. Scheffczyk, and W. Lauterborn, ''Bifurcation structure of bubble oscillators,'' J. Acoust. Soc. Am. **88**, 1061 (1990).

[41] V. Kamath and A. Prosperetti, ''Numerical integration methods in gas-bubble dynamics,'' J. Acoust. Soc. Am. **85**, 1538 (1989).

[42] N. A. Gumerov, ''Dynamics of vapor bubbles with non-equilibrium phase transitions in isotropic acoustic fields,'' Phys. Fluids. (submitted).

[43] N. A. Gumerov, personal communication.

[44] G. M. Patel, R. E. Nicholas, and R. D. Finch, ''Rectified heat transfer in vapor bubbles,'' J. Acoust. Soc. Am. **78**, 2122 (1985).

[45] P. L. Marston, ''Tensile strength and visible ultrasonic cavitation of superfluid ⁴He,'' J. Low Temp. Phys. **25**, 383 (1976).

[46] Van P. Carey, *Liquid-Vapor Phase-Change Phenomena* (Taylor & Francis, Washington, 1992).

[47] T. G. Theofanous, X. Chen, P. Di Piazza, M. Epstein, and H. K. Fauske, ''Ignition of aluminum droplets behind shock waves in water,'' Phys. Fluids **6**, 3513 (1994).